Journal of Power Sources 195 (2010) 2835–2843

Contents lists available at ScienceDirect

Journal of Power Sources

journal homepage: www.elsevier.com/locate/jpowsour

Optimizing the surfactant for the aqueous processing of $LiFePO_4$ composite electrodes

W. Porcher [a], B. Lestriez [b,*], S. Jouanneau [a], D. Guyomard [b]

[a] Commissariat à l'Energie Atomique, 38054 Grenoble Cedex 9, France
[b] Institut des Matériaux Jean Rouxel (IMN), Université de Nantes, CNRS, 44322 Nantes Cedex 3, France

ARTICLE INFO

Article history:
Received 2 April 2009
Received in revised form 21 October 2009
Accepted 20 November 2009
Available online 27 November 2009

Keywords:
Lithium battery
Electrode
$LiFePO_4$
Aqueous processing
Formulation
Surfactant

ABSTRACT

Aqueous processing would reduce the costs associated with the making of the composite electrode. To achieve the incorporation and the dispersion of the carbon black (CB) conductive agent in aqueous slurries, a surfactant is needed. In this paper, three surfactants are compared, an anionic one, the sodium dodecyle sulphate (SDS), a non-ionic one, the isooctylphenylether of polyoxyethylene called commercially Triton X-100 and a cationic one, the hexadecyltrimethylammonium bromide (CTAB), by using rheology and laser granulometry measurements on electrode slurries on one hand, and SEM observations, porosity and adhesion measurements and electrochemical testing on composite electrodes on the other hand. Ionic surfactants were found to be not suitable because a corrosion of the aluminium current collector occurred. The utilization of Triton X-100 favoured a more homogeneous CB distribution, resulted in a better electronic wiring of the active material particles and higher rate behavior of the electrode. Optimal electrochemical performances are obtained for an optimal surfactant concentration which depends on the BET surface area of the CB powder.

1. Introduction

An electrode for lithium-ion battery requires, around the active material grains, a percolating network of an electronic conducting agent, typically carbon black (CB), as well as a second percolating network of pores containing an ionic conducting electrolyte. In addition to the electronic conducting agent, the electrode is generally formulated with polymeric additives which must satisfy three main functions: (i) to disperse the powders, (ii) to confer rheological properties adapted for the technique of coating and (iii) to ensure the cohesion of the electrode and its adherence with the current collector [1]. The formulation generally employed for the positive electrode is made up of CB and a fluorinated polymeric binder, the poly(vinylidene fluoride) (PVdF). The use of this binder is due primarily to its electrochemical stability on a large potential window [2]. PVdF is insoluble in water and slurries are prepared industrially with an organic solvent, the N-methyl-pyrrolidone (NMP), that requires a process of recovery and treatment of the organic vapours.

Transition to an aqueous route, a more environmental friendly process, would reduce the costs associated with the making of the composite electrode, but new binder systems soluble in water and compatible with the requirements of a positive electrode of lithium-ion battery have to be found [2–9]. In this work we pursue two goals. First, we try to optimize an aqueous electrode formulation for the carbon-coated $LiFePO_4$ active material which is synthesized following a method developed by CEA (French Atomic Energy Commission) [10,11]; and second, we try to gain a more fundamental understanding on the mechanisms by which all polymers of the aqueous formulation, namely the thickener, the surfactant, and the binder operate, to be able to further generalize our study to other types of active materials. In two previous works, we assessed the stability of $LiFePO_4$ into water for standard processing conditions (pH, immersion time, solid loading) [12]; and we studied and selected carboxymethyl cellulose as the thickener [13]. Here, we are focused on the surfactant, which is incorporated into the aqueous electrode formulation to achieve the dispersion of the hydrophobic CB in water.

Surfactants are amphiphile chemical species, e.g. which have a hydrophobic group and a hydrophilic one. The hydrophobic group is generally a relatively short carbonaceous chain, meaning that the surfactant does not participate to the electrode cohesion or the electrode adhesion to the current collector. The hydrophilic group determines the ionic character of the surfactant. The carbonaceous chains adsorb themselves at the CB particle surface which enables to decrease the interfacial energy between water and CB and thus allows their dispersion in water. Several surfactants were selected

* Corresponding author at: Université de Nantes, CNRS, Institut des Matériaux Jean Rouxel (IMN), 2 rue de la Houssiniére, B.P. 32229, 44322 Nantes Cedex 3, France. Tel.: +33 2 4 03 739 32; fax: +33 2 40 37 39 95.
E-mail address: bernard.lestriez@cnrs-imn.fr (B. Lestriez).

0378-7753/$ – see front matter © 2009 Elsevier B.V. All rights reserved.
doi:10.1016/j.jpowsour.2009.11.088

in this study as a function of the charge sign of the hydrophilic group: (i) an anionic one, the sodium dodecyle sulphate (SDS), (ii) a non-ionic one, the isooctylphenylether of polyoxyethylene called commercially Triton X-100 and (iii) a cationic one, the hexadecyltrimethylammonium bromide (CTAB). As a recent example, Triton X-100 was observed to positively affect the dispersion of both CB and TiO_2 nanoparticles in NMP [14]. Here, the study to evaluate the more efficient surfactant began by optimising parameters of the implement of such additives (dispersion time and dispersion equipments). It was done from aqueous suspensions of CB with a fixed proportion of surfactant. Parameters were optimized according to laser granulometry characterizations. After having selected Triton X-100, more concentrated suspensions with various CB/surfactant ratios were then studied by rheology and laser granulometry. Effect on the CB particles dispersion was then evaluated by using these suspensions to prepare 3.0 mAh cm^{-2} $LiFePO_4$ electrodes whose morphology, adhesion to the current collector and electrochemical performance were characterized.

2. Experimental

2.1. Materials

The carbon-coated $LiFePO_4$ active material used was prepared according to Refs. [15,16]. A mechanochemical activation was performed using commercial Li_3PO_4 and fresh iron(II) phosphate as the source of the main components and the electronic conductor additive precursor (sucrose for a carbon coating) was incorporated initially with the two reactants. The powders were ball milled in a planetary mill (Retsch S1000) with agate vessels. The resulting product was then heat-treated at 800 °C under nitrogen and rapidly cooled. This thermal treatment is necessary to crystallize the final compound $LiFePO_4$ and to form the desired coating around the particles. This $LiFePO_4$ has a carbon content of about 3 wt.%, and a specific surface of 20 $m^2\,g^{-1}$. The size of the primary particles is in the [60–100 nm] range [12]. They are agglomerated into secondary particles with a mean diameter of 17 μm. Particle size distribution can be found in Ref. [13]. XRD pattern is that of pure $LiFePO_4$ [17].

The carbon black used is a Carbon Super P™ from *Timcal* with a specific surface of 60 $m^2\,g^{-1}$. Aqueous suspensions of CB were prepared with deionized water (with $\sigma = 50\,\mu S\,cm^{-1}$) and various surfactants, the sodium dodecyle sulphate (SDS from *Aldrich*, $M_{SDS} = 288\,g\,mol^{-1}$), the isooctylphenylether of polyoxyethylene (Triton X-100 from *Aldrich*, $M_{Triton\ X\text{-}100} = 652\,g\,mol^{-1}$) and the hexadecyltrimethylammonium bromide (CTAB from *Aldrich*, $M_{CTAB} = 364\,g\,mol^{-1}$). The binders used were a mix of polyvinyl alcohol (PVA, $M_w = 78{,}000$–88% hydrolysed, *Polysciences*) and polyethylene glycol (PEG, $M_w = 400$, *Aldrich*); or a butadiene–acrylonitrile copolymer rubber latex, NBR; or a poly(vinylidene fluoride) (Solef PVdF 6020, *Solvay*). The two thickeners used were a hydroxyl propyl methyl cellulose (HPMC, 1.8–2.0 mol methoxy per mol cellulose, 0.2 mol propylene oxide per mol cellulose, $M_n = 86{,}000$, *Aldrich*) and a carboxyl methyl cellulose (CMC, 0.7 mol carboxyl per mol cellulose, $M_w = 250{,}000$, *Aldrich*).

2.2. Characterization of the slurries

Rheological properties of CB aqueous suspensions were measured on a controlled-stress rotating rheometer (MCR 300, *Anton Paar*) with a 50 mm diameter plane-and-plane geometry, with a sample gap between the Pelletier plane and the geometry ranging of about 1 mm. Drying of the sample during the measurement was prevented by using the classical *solvent trap* accessory. Before measurement started, the sample was equilibrated at 25 °C. As generally observed, we found that for a good reproducibility of the measurements, it was necessary to pre-shear the sample (here at 1000 s^{-1} for 45 s), and then to let it rest (here for 1000 s). It ensures that all samples have the same mechanical history. Viscosity or shear stress is then measured as a function of the shear rate from 1000 to 0.1 s^{-1} to determine viscosity. Particles size distribution in dilute medium was measured by low angle laser light scattering using a Mastersizer S laser granulometer (*Malvern*). A drop of CB aqueous suspension was diluted in 100 mL of deionised water before measurement.

2.3. Preparation of composite electrodes

Electrode slurries were prepared in deionized water (aqueous processing) or non-aqueous processing (NMP) with a high-speed mixer that was used to shear the electrode slurry for 10 min. The slurry was then tape cast by using an automatic doctor blade onto an aluminum current collector. The thickness of the gap between the blade and the current collector was fixed to 100 and 600 μm, resulting in 0.5 and 3.0 mAh cm^{-2} surface capacity, respectively. Drying was primarily done at 55 °C. Electrodes were then pressed under 2 tons cm^{-2}. Before battery assembly, a further drying at 80 °C under dynamic vacuum was done.

2.4. Characterization of the electrodes

Scanning electron microscopy (SEM) imaging and energy dispersive X-ray chemical mapping was performed on gold–palladium sputtered samples using, respectively, a JEOL JSM 7600F apparatus and a QUANTAX EDS from BRUKER. Cryogenic fractures were used to image the cross-section of the sample. The elemental spatial distribution of phosphorus, iron and carbon were observed on the same but carbon sputtered samples.

Adhesion between the electrode and the current collector was estimated as follows. Electrodes are densified step by step with a pressure that is increased progressively. After each step, the height of the electrode is also measured, from which the porosity can be calculated by using the mass and the density of the electrode constituents. When the electrode delaminates from the current collector, the pressure applied at the previous step is taken as a practical limiting value which reflect adhesion between the electrode and the current collector, and the minimum porosity achievable is defined.

$LiFePO_4$-based composite electrodes were assembled in electrochemical cells with lithium metal as counter electrode, Celgard film as separator soaked in an electrolyte consisting of a 1 M $LiPF_6$ solution in an ethylene carbonate-dimethyl carbonate (EC-DMC 1/1) mixture. The assembly of the button cells was carried out in a dry glove box under argon atmosphere. Electrochemical experiments were performed at 20 °C, monitored by an Arbin instrument, between 2.0 and 4.2 V versus Li^+/Li, by beginning by two slow charge–discharge cycles at *C*/10 rate. Successive discharges from 30*C* to *C*/50 rate, interrupted with only relaxation times for 30 min, were then repeated many times after a charge at *C*/10 rate. Results for second successive discharges are kept to compare electrodes.

3. Results and discussion

3.1. Implement and selection of the surfactant

Aqueous CB suspensions with 3 wt.% of CB and $1.5 \times 10^{-2}\,mol\,L^{-1}$ of surfactant were elaborated to determine the influence of the dispersion time and the type of dispersion equipment on the distribution in volume of CB particle sizes in the presence of a surfactant. This surfactant/CB ratio was chosen for these first tests according to the literature [18–20]. First of all, Fig. 1,

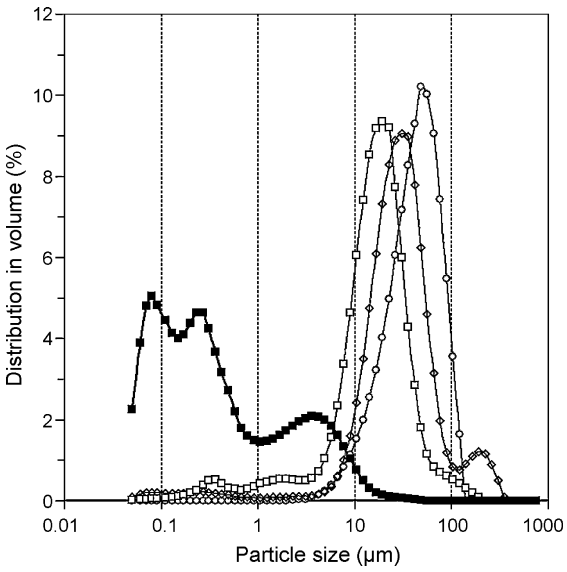

Fig. 1. CB particle size distribution according to the process implemented and mixing time: 24 h of soft mixing on a roller bank (■) or 30 min of energetic mixing (ball milling (□), high-speed mixer (○), and their combination (◊)), for suspensions containing 3 wt.% CB and 1.5×10^{-2} mol L^{-1} of Triton X-100.

it appears that surfactants positively affect the CB dispersion only after a certain lap of time. It is indeed preferable to let agitate the suspension at least 24 h, even with a soft mixing of the type roller bank or magnetic stirrer, for example. With a high energy mixing device, ball milling or high-speed mixer or their combination, it seems difficult to obtain aggregates lower than 10 μm after 30 min of treatment of the suspension, whereas after 24 h of soft milling, a very important nanometric population is obtained. Thus the CB dispersion will have to be carried out upstream.

The CB particle size distributions obtained for each of the three surfactants after 24 h of soft mixing are presented in Fig. 2. Firstly, one can note that these distributions do not show anymore the presence of giant agglomerates of several tens of microns. These ones are dispersed as nanometric particles. The distributions with the Triton X-100 non-ionic surfactant and the CTAB cationic surfactant are rather similar. On the other hand the SDS anionic surfactant

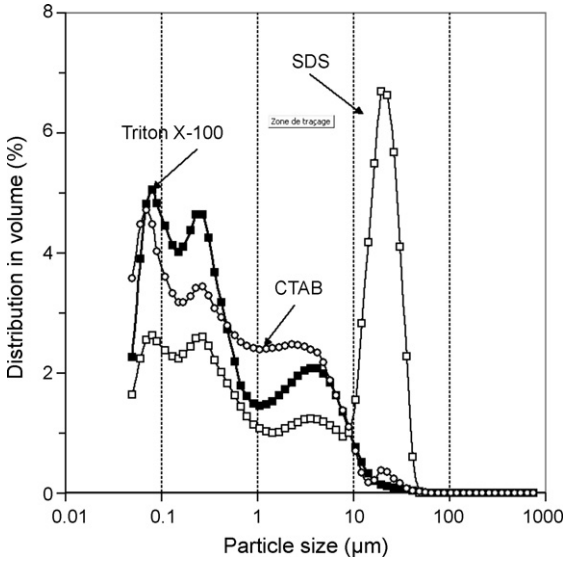

Fig. 2. CB particle size distribution following the nature of the surfactant, anionic SDS (□), non-ionic Triton X-100 (■), cationic CTAB (○), for suspensions containing 3 wt.% CB and 1.5×10^{-2} mol L^{-1} of Triton X-100.

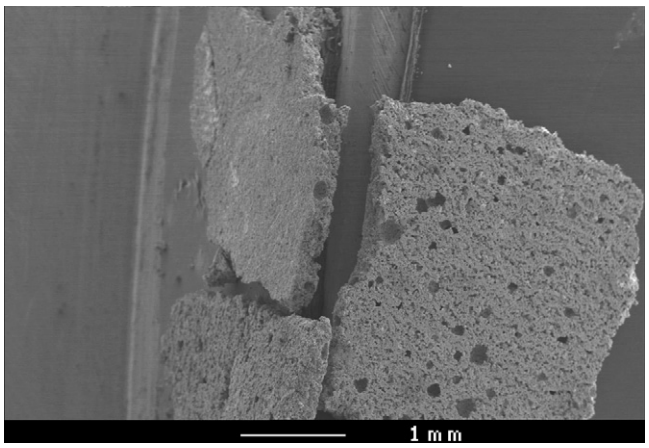

Fig. 3. SEM picture of pieces of an electrode elaborated with an ionic surfactant (1.5 wt.% of surfactant).

seems less effective, as one can note an important micrometric population centered on 20 μm.

The pHs of the CB suspensions are 4.5, 6.5 and 9.3 for the suspensions of CTAB, Triton X-100 and SDS, respectively. Previous works have shown that the pH of $LiFePO_4$ suspensions should not be modified and that the natural pH of the $LiFePO_4$-base suspension is about 9 [12]. Therefore, we will choose for continuation, after having eliminated the less efficient SDS, the Triton X-100 because the CTAB is better appropriated for an acid medium given the sign of its charge and its natural pH.

Moreover when electrodes were elaborated with CB dispersed with an ionic surfactant, either SDS or CTAB, a very marked pitting could be observed on the aluminum collector. The produced electrodes also show cavities of important size on their current collector side, Fig. 3, which could be associated with a hydrogen release, reveals corrosion of current collector by the slurry. Thus, as a general rule, the ionic surfactants appear to be not viable for the application aimed with an aluminum collector because of their chelating capacities. Thus only the non-ionic surfactant, the Triton X-100 from now on will be definitively considered. Nevertheless the particle size distribution achieved for CB is quite interesting when one compares it to the distribution of $LiFePO_4$ particle sizes, Fig. 4, and the prediction of Malliaris et al. [21]. Indeed, Eq. (1) gives the critical volume fraction of the conductive material to reach electrical percolation in a conductor/insulator composite material, here our electrode:

$$\phi_c = \left(1 + \frac{3}{4}\frac{R_i}{R_c}\right)^{-1} \quad (1)$$

with Φ_c, the critical volume fraction of the electronic conductor, here CB, which depends on the diameters of the conducting particles, R_c, and of the insulating particles, R_i, here $LiFePO_4$. According to the values of the mean diameter, D_{50}, of the particles, 270 nm and 17 μm for the aqueous suspension of CB with Triton X-100 and that of $LiFePO_4$, respectively, one predicts a critical CB volume fraction of ~2 vol.% which corresponds to a critical CB weight fraction of ~1 wt.%, by considering the respective densities of the two materials (3.57 for $LiFePO_4$ and 1.8 for CB) and a typical porosity (see Section 2.2) of 35 vol.%.

The Triton X-100 efficiency can also be evaluated by comparing the particle size distributions obtained for a suspension of CB with 20 g L^{-1} of HPMC but without Triton X-100 (Fig. 4). HPMC was the thickening agent defined a priori for our study. Another recent publication of our group demonstrates that carboxymethyl cellulose (CMC) is more efficient as thickening agent [13]. Here, HPMC is observed to allow the incorporation of the CB in water, likely due to

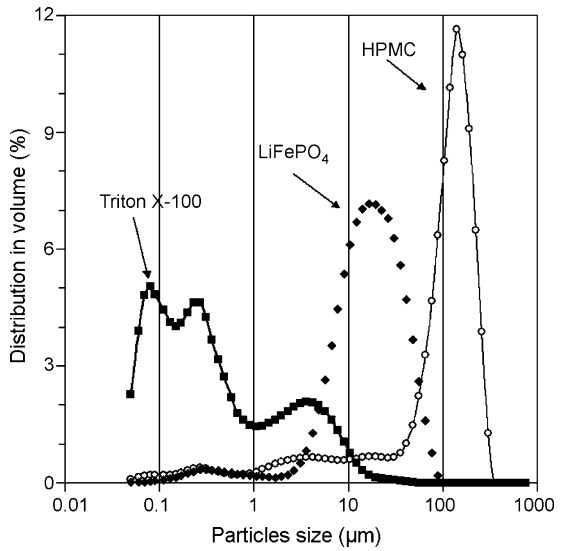

Fig. 4. Distributions of particle sizes for aqueous suspensions with 3 wt.% of CB and 1.5×10^{-2} mol L^{-1} of Triton X-100 (■) or 20 g L^{-1} of HPMC (○) prepared according to the protocol optimized for the surfactant. Distribution in volume of the particle size of $LiFePO_4$ (♦).

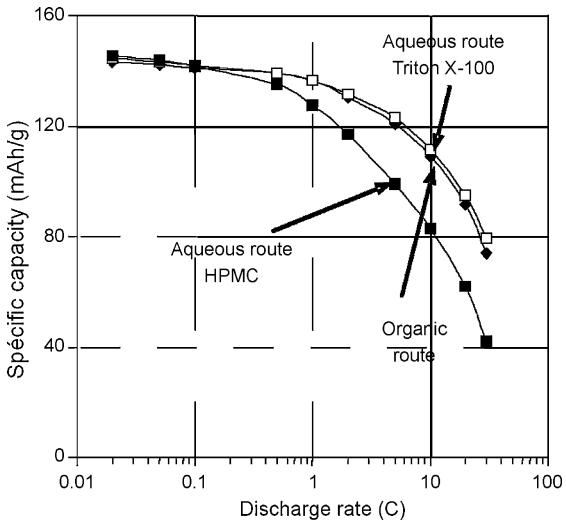

Fig. 5. Specific capacities (discharge capacity given per mass of active material) at different discharge rates from *C*/50 to 30*C* of ~0.5 mAh cm^{-2} PVdF (♦), HPMC (■), Triton X-100 (□) electrodes.

the adsorption of these chains on the CB particles which lowers the free energy at the CB/water interface. The particle size distribution of CB in this suspension without Triton X-100, however, shows a significant fraction of giant agglomerates, roughly equal to 80% of the total volume of CB.

The electrochemical performance, in terms of specific capacities at different discharge rates from *C*/50 to 30*C*, of "thin electrodes" (loading around 0.5 mAh cm^{-2}) prepared with HPMC and with or without Triton X-100 are shown in Fig. 5 and compared to the one of a classical electrode (poly(vinylidene fluoride)) binder (PVdF) prepared in N-methyl pyrrolidone. Compositions are reported in Table 1. The aqueous processed electrode whose formulation does not contain Triton X-100 has significantly lower performance at high rate, while the one which contains Triton X-100 behaves similarly to the non-aqueous one. These results show that it is possible to obtain satisfactory results in aqueous way, with an important proportion of active material, when CB particles are well dispersed.

3.2. Optimization of the surfactant concentration

3.2.1. Study of composite electrode slurries

Note that in this section, for practical reasons, to elaborate electrode slurries with an optimal solid loading, suspensions of CB have being concentrated from 3 to 5 wt.%. However, the CB content in dried electrodes is the same (see Table 1).

Work of Gonzalez-Garcia et al. [20] describes rather well the adsorption of Triton X-100 on six different CB with specific surface from 37 to 1443 m^2 g^{-1} in diluted suspensions. From calculations on the free energy of adsorption and steric hindrance considerations, the authors showed that the adsorbed part of the surfactant corresponds to the carbonaceous chain as well as the phenol group and 2 or 3 oxy ethylene groups of the Triton X-100 chain. This portion of the Triton X-100 molecule occupies a surface area of 1.48 nm^2. Besides, it can be deduced from their work that full coverage of the CB surface by a Triton X-100 monolayer corresponds to an adsorbed surfactant amount of approximately 1.12 μmol m^{-2}. It should be noted that the surfactant adsorption is reversible. Then, there is a balance between the free surfactant in the solution and the one adsorbed. The surfactant concentration in the solution to reach the situation of full coverage depends on the CB specific surface and the solid loading in the suspension. In the study of Gonzalez-Garcia et al., it can be observed that at equilibrium, i.e. when a Triton X-100 monolayer covers all the particles, approximately one-third of the surfactant amount is adsorbed while two-third remains in the liquid phase. This allows calculating the limiting concentration of Triton X-100 to add into the slurry to reach full coverage of the CB particles. In this part, suspensions of CB with a solid loading of 5 wt.% have been used. Thus, in 1 L of CB suspension, given its specific surface of 60 m^2 g^{-1}, the amount of adsorbed Triton X-100 at full coverage is 1.12 μmol m^{-2} × 60 m^2 g^{-1} × 50 g = 3.36 mmol. And it would remain in the solution 6.72 mmol. The total amount of Triton X-100 introduced in the CB suspension (1 L) being thus 10.08 mmol, or 6.6 g L^{-1}. In the following, we have studied the effect of the surfactant concentration in the CB suspension on the dispersion of the CB and thereafter on the morphology, adhesion and electrochemical performance of the corresponding electrodes. The studied Triton X-100 concentrations in the CB suspension are 1, 5, 10 and 15 g L^{-1}, which corresponds to 0.1, 0.5, 1 and 1.5 wt.% in the dried electrodes.

Table 1
Electrode composition and surface capacity density.

Electrodes	Surface capacity density (mAh cm^{-2})	$LiFePO_4$ (wt.%)	CB (wt.%)	PVdF (wt.%)	Triton X-100 (wt.%)	HPMC (wt.%)	CMC (wt.%)	$PVA_{0.7}$ $PEG_{0.3}$ (wt.%)	NBR (wt.%)
PVdF	0.5	80	10	10	–	–	–	–	–
HPMC	0.4	91	5	–	–	2	–	2	
HPMC TX-100	0.5	89.5	5	–	1.5	2	–	2	
(CMC TX-100)-1	3.0	90.9	5	–	0.1	–	2	–	2
(CMC TX-100)-2	3.0	90.5	5	–	0.5	–	2	–	2
(CMC TX-100)-3	3.0	90	5	–	1.0	–	2	–	2
(CMC TX-100)-4	3.0	89.5	5	–	1.5	–	2	–	2

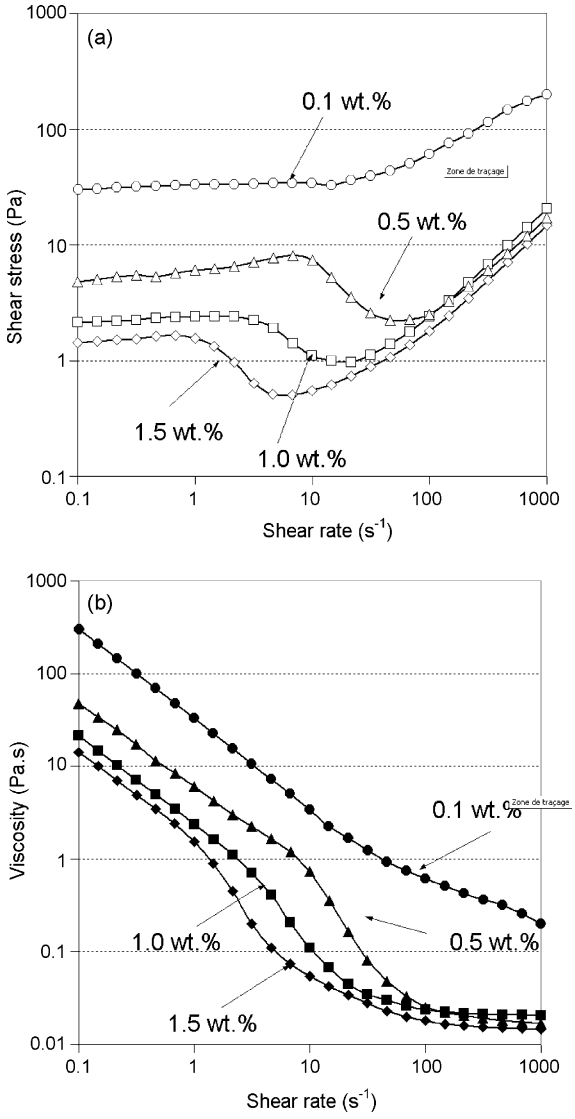

Fig. 6. (a) Shear stress τ and (b) viscosity η as a function of the shear rate for aqueous suspensions containing 5 wt.% of CB and varying proportions of surfactant TX100, 1 g L^{-1} (●, ○), 5 g L^{-1} (▲, △), 10 g L^{-1} (■, □) and 15 g L^{-1} (♦, ◊).

The rheological behavior of the CB suspensions was studied for the different Triton X-100 concentrations. The shear stress τ and the viscosity η versus the shear rate is given in Fig. 6. A shear-thinning behavior is observed in all cases, i.e. a decrease of the viscosity with increasing shear rate. This is typical of flocculated dispersions where the presence of weak attractive forces between the particles leads to the formation of clusters of particles (including enclosed solvent) called flocs. At high shear rate, the occurrence of a limiting constant value of the viscosity suggests the viscous stresses of the solvent on the CB agglomerates are sufficient to fully break them apart so that only the primary aggregates remain. However, at low shear rate, all suspensions show a plateau on the shear stress curve. The corresponding value of τ is called yield stress, noted τ_0 and is the manifestation of a self-supporting network of interconnected flocs throughout the system. The yield stress τ_0 is a measure of the strength of the network or the connectivity of the flocs of particles, which depends, among others, on the strength of the attractive interactions between the particles [22]. Fig. 6a shows the yield stress decreases as the surfactant concentration is increased, demonstrating a progressive weakening of the attraction between the particles of CB as the Triton X-100 concentration is increased

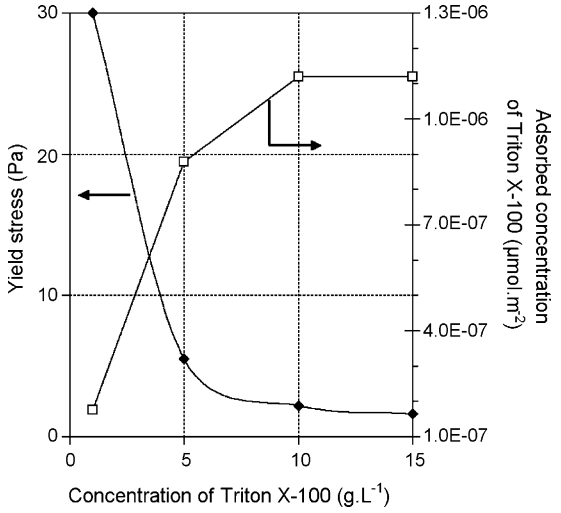

Fig. 7. Variation of τ_0 and of the theoretical amount of adsorbed Triton X-100 as a function of the initial Triton X-100 concentration in the CB suspensions.

from 1 to 15 g L^{-1}, with almost no variation from 10 to 15 g L^{-1}. Fig. 7 compares the variation of τ_0 with the theoretical variation of the amount of Triton X-100 adsorbed as a function of the Triton X-100 concentration. The former data are a rough extrapolation from the work of Gonzalez-Garcia et al., where we considered that one-third of the surfactant adsorbs while two-thirds remain like free molecules in the liquid phase of the suspension until the equilibrium state of full coverage of the particles by a Triton X-100 monolayer is reached. Fig. 7 clearly illustrates that the decrease of the CB interparticle attraction and of their agglomeration is a direct consequence of the adsorption of Triton X-100 at the surface of the particles until a Triton X-100 monolayer is reached.

Distribution of the particles size for the same CB suspensions is presented in Fig. 8. For the suspension containing 0.1 wt.% of surfactant, the distribution is coarse since no nanometric population exists while agglomerates of several hundred microns can be observed. Contrarily, an important nanometric population is observed for the suspensions containing 0.5, 1.0 and 1.5 wt.% of surfactant. The volume fraction of the nanometric population increases

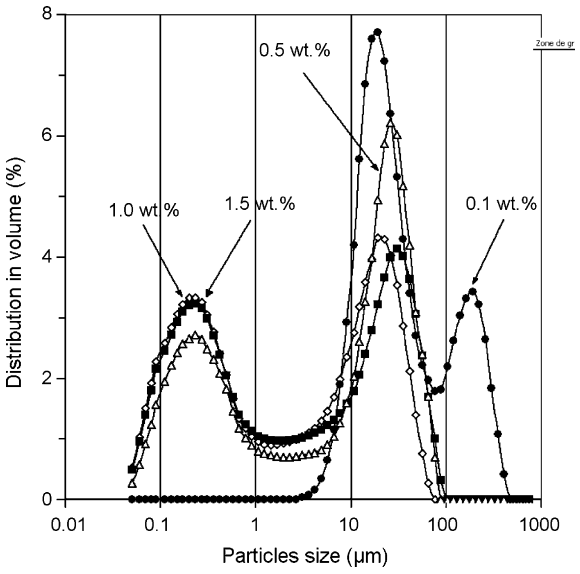

Fig. 8. Distribution of the particles size for aqueous suspensions containing 5 wt.% of CB and variable Triton X-100 proportions, 0.1 wt.% (●), 0.5 wt.% (△), 1.0 wt.% (■) and 1.5 wt.% (◊).

with the surfactant concentration, respectively, 35, 43 and 45% in volume, in fairly good correlation with the variation of the yield stress of the CB suspensions and the theoretical amount of surfactant adsorbed at the surface of the CB particles. A decrease of the yield stress and an increase of the volume fraction of the nanometric population are observed with an increase of the surfactant until the point where the situation of full coverage is reached; at this point the yield stress and the volume fraction of the nanometric population no more evolve. Additionally, one can observe that compared to the suspensions studied in the first part of this paper with 3 wt.% of CB (Fig. 2) the volume fraction of the micrometric population is higher, certainly due to the fact that the distance between the particles inside the suspension is reduced, due to a higher concentration of particles, which favours their agglomeration. Finally, one can note that the rheological measurements show that the CB suspensions are weakly flocculated even when the Triton X-100 concentration is such that theoretically the equilibrium state of full coverage of the CB primary aggregate surface is reached. The shear-thinning character shows that the state within the suspension is a mixture of individual primary aggregates and agglomerates of

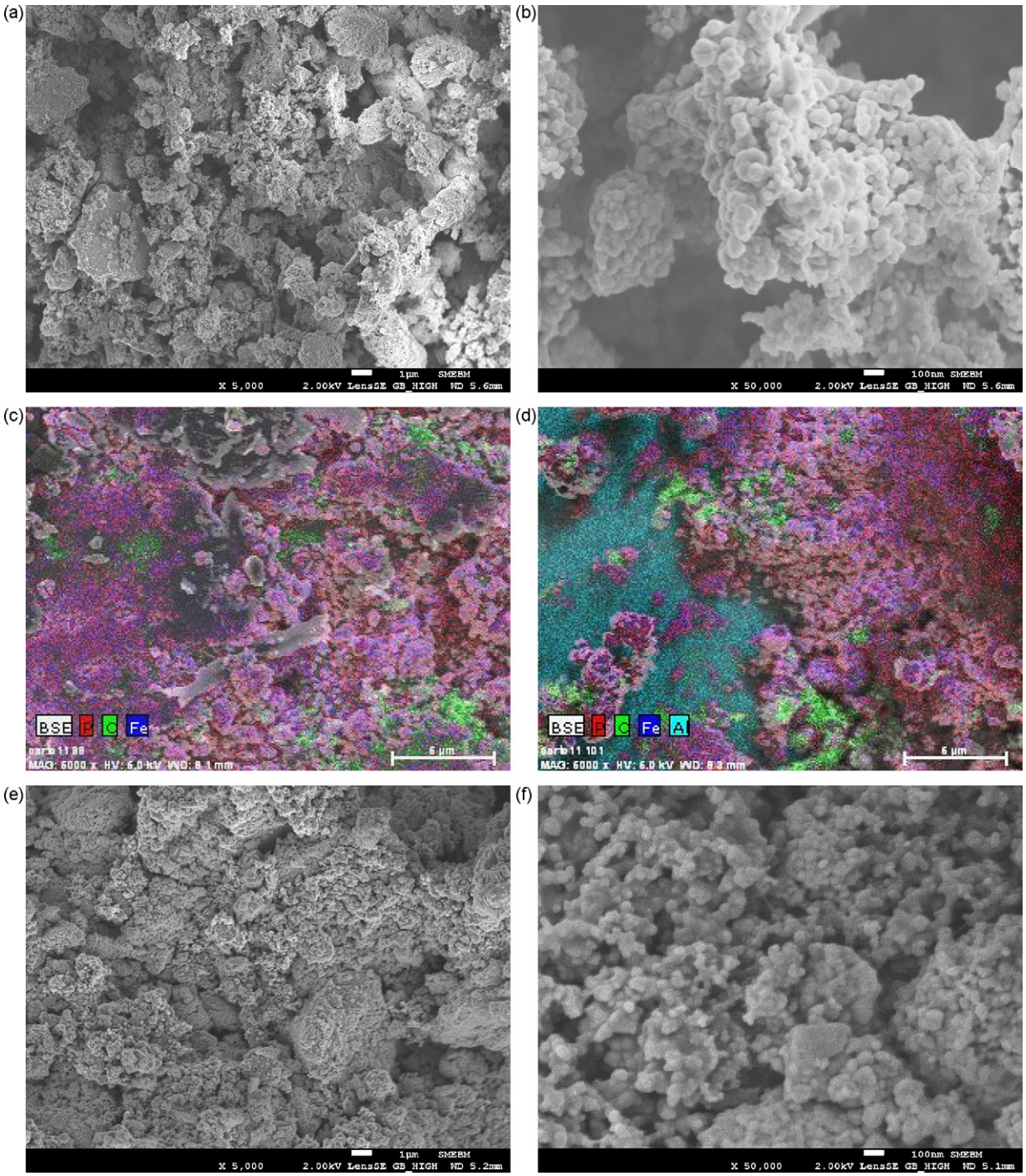

Fig. 9. SEM observation of 3.0 mAh cm^{-2} electrodes containing (a and b) 0.1 wt.% and (e and f) 1.5 wt.% Triton X-100. Typical phosphorus, iron and carbon spatial distributions in the same electrodes (c and d) 0.1 wt.% and (g and h) 1.5 wt.% Triton X-100. The pink color reveals $LiFePO_4$, the intense green color CB, and the pale green color the binder. Turquoise blue reveals the aluminum current collector (c). (For interpretation of the references to color in this figure legend, the reader is referred to the web version of the article.)

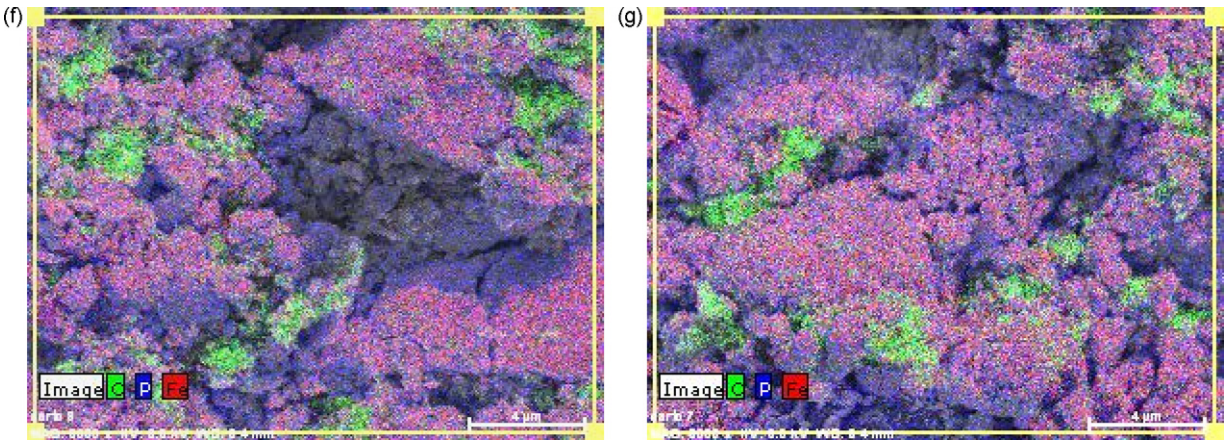

Fig. 9. (*Continued*).

them, as reflected by the laser granulometry measurements, the size of the agglomerates varying with the shear rate.

3.2.2. Study of composite electrode films

Morphology within the dried composite electrodes depends on the surfactant concentration (Fig. 9). SEM observations of films calendared below 2 tons cm^{-2} show that in the electrode containing 0.1 wt.% of Triton X-100, the architecture is constituted by large blocks that look strongly stuck to each other delimiting large pores of more than a 1 μm in size (Fig. 9a). Pictures taken at a higher magnification reveal that these blocks are made of $LiFePO_4$ secondary particles (50–100 nm ellipsoidal primary particles) (Fig. 9b). CB (about 50 nm spherical primary particles) was hardly detectable. In the electrode containing 1.5 wt.% of Triton X-100, the architecture appears to be a much more intimate mixture of $LiFePO_4$ secondary particles and CB small agglomerates, Fig. 9e and f, delimiting small pores of hundred of nm in size. Because of the fairly close appearance of both types of grains, i.e. $LiFePO_4$ and CB, it was, however, very difficult to characterize more quantitatively the homogeneity of the CB distribution. Thus, the spatial distributions of the phosphorus, iron, carbon and aluminum (current collector) elements were measured in complement by using spatially resolved energy dispersive X-ray microanalysis, Fig. 9c, d, g and h. In the electrode containing 0.1 wt.% of Triton X-100, these measurements reveal the occurrence of large depleted or rich, CB zones, Fig. 9c and d, while in the electrode containing 1.5 wt.% of Triton X-100, CB could be detected as small agglomerates of mostly 1 μm size with a fairly homogeneous distribution, Fig. 9g and h, residing in the interstice between $LiFePO_4$ secondary particles. One note that the dimension of the CB agglomerates in the electrode containing 0.1 wt.% of Triton X-100 is smaller, while in the electrode containing 1.5% of Triton X-100 it is bigger, than what could be expected from the laser granulometry measurements, i.e. hundred of μm and hundred of nm for 0.1 wt.% and 1.5% of Triton X-100, respectively. The latter measurements were done on model CB suspensions without all other constituents of the electrode. The addition in the suspending medium of the thickener, the binder, and of the $LiFePO_4$ secondary particles is indeed likely to play a role on the CB distribution. Nevertheless, qualitatively, the CB distribution within the composite electrode films with different surfactant content appear in good agreement with the state of the CB distribution within the corresponding CB suspensions.

Adhesion between the electrode and the current collector was estimated in order to determine whether the surfactant is detrimental or not on this critical property. Several mechanical tests exist to characterize adhesion between a current collector and an electrode. Some of them are qualitative such as the "scratch off" test that uses a flat knife to scratch off the electrode film from the current collector [23] or such as the "peel-off" test that uses a calibrated scotch tape to peel off the electrode film from the current collector [3]; others try to be more quantitative by measuring a value of the adhesion strength from a force gauge with various geometry of the sample and the experimental set-up [4,24,25]. We have used a practical method. After drying, commercial electrodes are usually pressed down to about 30–40 vol.% porosity. It is accepted that this treatment is essential for obtaining simultaneously high energy, high rate and good cycling stability. Adhesion is critical with respect to the calendaring step, as the electrode must not delaminate from the current collector at this time. Thus, we have measured, as a function of the surfactant content for "thick electrodes" (loading around 3 mAh cm^{-2}), Fig. 10a and b, the maximum calendaring pressure that can be loaded on the electrode and the minimum achievable porosity of the electrode. Both quantities are particularly different for the electrode with 0.1 wt.% of surfactant compared to the others. For 0.1 wt.% of surfactant, the maximum calendaring pressure reaches 4 tons cm^{-2} and the minimum achievable porosity 25%, while they are in between 2 and 2.5 tons cm^{-2} and 35–40% for the three others surfactant concentration, i.e. 0.5, 1, and 1.5 wt.% (Fig. 10a). Laser granulometry measurements allow to calculate the total apparent surface area from the particle size distribution and considering spherical particles from the following expression:

$$S_{\text{apparent}} = \sum_i \phi_i \frac{6}{d_i \rho} \tag{2}$$

where ϕ_i is the volume fraction of the particles or agglomerates of diameter d_i and ρ is the density (in g per cm^3). The sum of the total apparent surface area of the CB and $LiFePO_4$ powders (weighted by their mass fraction, see Table 1) strongly varies with the surfactant concentration and is 0.04, 0.36, 0.47 and 0.48 m^2 per gram of electrode for 0.1, 0.5, 1 and 1.5 wt.% of Triton X-100, respectively (Fig. 10b). The maximum applicable calendaring pressure decreases and the minimum achievable porosity increases with S_{apparent} of the powders. This can be explained using the recent models developed for fracture of polymer interfaces [26]. Interfacial toughness is controlled by the strength of the polymer bridges that cross the interface:

$$\sigma_{\text{int}} = f_b \Sigma \tag{3}$$

where Σ is the area density of connecting chains that are anchored on both sides of the interface and cross over the interface, and f_b is the strength of the anchoring bond or the force to break a covalent bond in the polymer chain if the latter is weaker than the former. Here, the total surface area increases with the surfactant concentration as the volume fraction of the nanometric

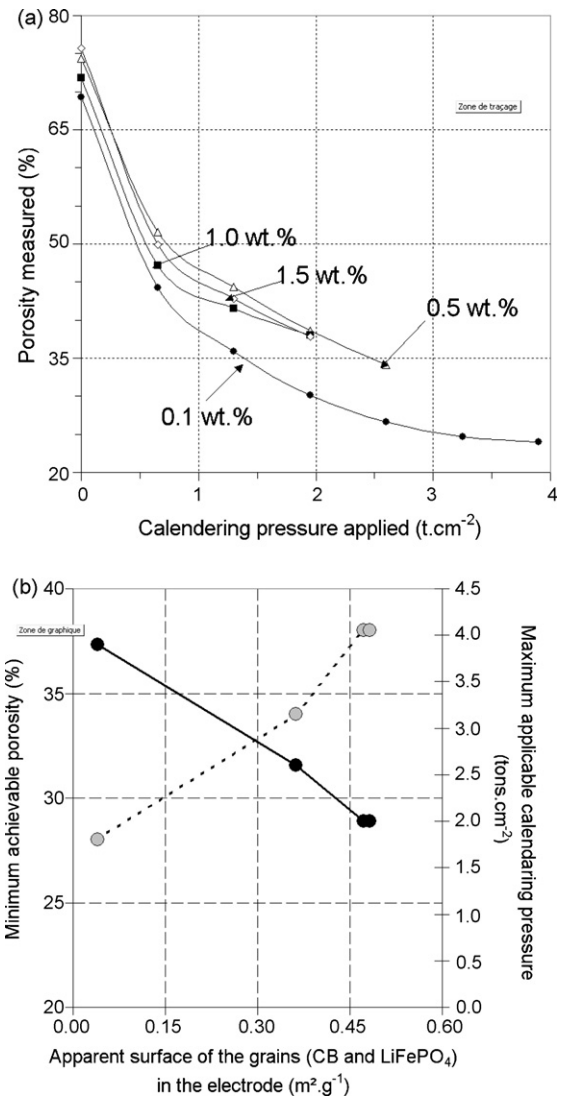

Fig. 10. (a) Evolution of the porosity as a function of the calendaring pressure for 3.0 mAh cm^{-2} electrodes containing $(91-x)$wt.% of $LiFePO_4$, 5 wt.% of CB, x wt.% of Triton X-100, 2 wt.% of NBR and 2 wt.% of CMC, with x = 0.1 wt.% (●), 0.5 wt.% (△), 1.0 wt.% (■) and 1.5 wt.% (◊). (b) Minimum achievable porosity and maximum applicable calendaring pressure as a function of the apparent surface of the grains (CB + $LiFePO_4$) and corresponding surfactant concentration in the dried electrode.

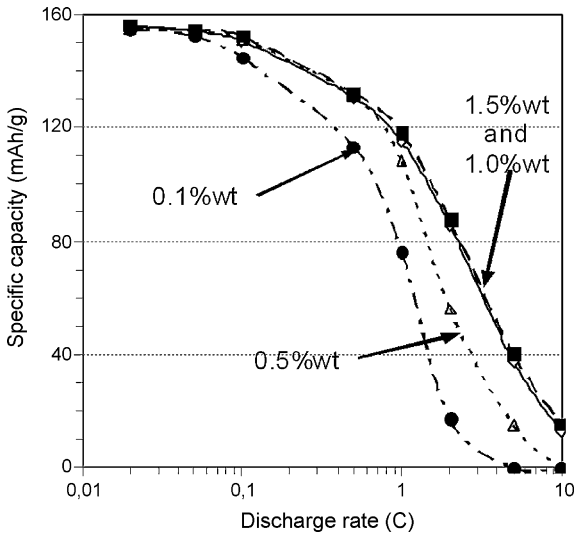

Fig. 11. Specific capacities of electrodes of 3.0 mAh cm^{-2} containing $(91-x)$wt.% of $LiFePO_4$, 5 wt.% of CB, x wt.% of Triton X-100, 2 wt.% of NBR and 2 wt.% of CMC, with x = 0.1 wt.% (●), 0.5 wt.% (△), 1.0 wt.% (■) and 1.5 wt.% (◊).

population increases in the CB particle size distribution. Thus, if we assume an homogeneous distribution of the binder, then the area density of connecting chains Σ decreases when the surfactant concentration increases. Thus, a drawback of adding the Triton X-100 is to decrease the adhesion between the electrode and the current collector. In a further work this property will be improved. However, coming back to this study and to the further electrochemical measurements, we stress that electrodes where calendared up to 2 tons cm^{-2}. Porosity is the same for electrodes containing 0.5, 1.0 and 1.5 wt.% of surfactant at this calendaring pressure, i.e. 37%, while it is fairly lower for 0.1 wt.%, i.e. 30%.

The electrochemical performance of "thick electrodes" (loading around 3 mAh cm^{-2}) with various surfactant contents (Table 1) is compared in Fig. 11. For all these electrodes, discharge capacities at a current rate superior to 0.5*C* are reduced compared to those obtained for the "thin electrodes", which is a behavior allotted mainly to a slower ionic conduction of the lithium ions in the electrolyte within the electrode when its thickness increases [27,28]. At low current rate, the electrodes have the same discharge capacities, which indicate that all the active material particles are wired to the electronic collation web. However, above a current rate of 0.1*C*, the electrochemical performance follows the CB dispersion state, i.e. the discharge capacity increases until 1 wt.% of Triton X-100 as does the volume fraction of the nanometric population of CB particles within the CB suspension. Because the porosity of the composite electrode is the same from 0.5 to 1.5 wt.% of surfactant, it is likely that the variation of the discharge capacity for these electrodes is due to differences in the electronic wiring of the active particles and rather than in the ionic wiring.

To assess which of the electronic or ionic parameter is limiting the lithium intercalation/deintercalation in Li_xFePO_4, we have measured from cycling experiments the polarization at 50% of the state of the charge (SOC) between discharge and charge curves. At this SOC, for low rate, discharge and charge curves are flat voltage region characteristic of a two-phase system and the polarization between charge and discharge curves can be precisely determined (Table 2). For charge and discharge rates of 0.1*C*, results show that polarization is significant higher for electrodes containing 0.1 and 0.5 wt.% of Triton X-100. It is generally well accepted that at low rate, lithium-ion diffusion inside liquid electrolyte is not a limiting factor. Therefore, these results confirms that from 0.5 to 1.5 wt.% of Triton X-100, the improvement of the CB distribution results in a better electronic wiring and higher electrochemical performance in power. At very low surfactant concentration, i.e. 0.1 wt.% of Triton X-100, the electronic wiring is likely to be very poor. Moreover, because porosity is fairly low, i.e. 30%, it is possible that the very poor electrochemical performance could also arise from lower ionic conductivity.

Finally, the optimal surfactant concentration of 1.0 wt.% corresponds to the situation of full coverage of the surface of the CB particles with one monolayer of Triton X-100. Above this concentration, the CB distribution and the electrochemical performance were not improved.

Table 2
Electrode polarization between charge and discharge curves at 50% of SOC as a function of the surfactant content inside the electrode.

Rate	Surfactant content inside the electrode			
	0.1 wt.%	0.5 wt.%	1.0 wt.%	1.5 wt.%
0.1*C*	170 mV	120 mV	100 mV	105 mV

For further works, the effect of the surfactant on the cycling behavior of the $LiFePO_4$ electrode at different temperatures and on the possible surface layer are open questions.

4. Conclusion

A surfactant is needed to disperse the CB electronic conductor and obtain a satisfactory aqueous processing of a $LiFePO_4$ composite electrode for lithium battery. Ionic surfactants were found to be unsuitable because they are observed to induce the corrosion of the aluminium current collector. The isooctylphenylether of polyoxyethylene (Triton X-100) is an efficient non-ionic surfactant which can be used for the purpose. Optimization of the implementation of this surfactant shows that CB aqueous suspensions must be carried out upstream (24 h before use) to achieve a good balance between surfactant adsorbed at CB particles surface and free surfactant in solution. Rheological measurements or laser granulometry experiments can be employed to tailor the surfactant concentration. A decrease of the yield stress of the CB suspension and an increase of the volume fraction of the nanometric population in the CB particle size distribution are observed up to the point where full coverage is reached. This situation corresponds to an adsorbed surfactant amount of 1.12 μmol m^{-2}, with at least two-thirds of the total amount of surfactant remaining as free molecules in the liquid phase of the suspension. Improvement of the CB dispersion in the electrode slurries results in more homogeneous CB distribution within the dried composite electrode and better electronic wiring of the active material particles, leading to higher discharge capacity at high rate. Optimal electrochemical performances are obtained for a surfactant concentration such that the situation of full coverage of the CB surface by a Triton X-100 monolayer is reached in the electrode slurry.

Acknowledgments

W.P. gratefully acknowledge ADEME (Agence De l'Environnement et de la Maîtrise de l'Energie) and CEA/INSTN (Commissariat à l'Energie Atomique/Institut National des Sciences & Techniques Nucléaires) for financial support.

References

[1] B. Lestriez, E. Ligneel, D. Guy, D. Guyomard, in: S.S. Shui (Ed.), Advanced Materials and Methods for Lithium-Ion Batteries, Transworld Research Network, Kerala, India, 2007, (Chapter 10).
[2] A. Guerfi, M. Kaneko, M. Petitclerc, M. Mori, K. Zaghib, J. Power Sources 163 (2) (2006) 1047.
[3] S.S. Zhang, K. Xu, T.R. Jow, J. Power Sources 138 (2004) 226.
[4] J.-H. Lee, U. Paik, V.A. Hackley, Y.-M. Choi, J. Power Sources 161 (2006) 612.
[5] J.-H. Lee, G.-S. Kim, Y.-M. Choi, W.I. Park, J.A. Rogers, U. Paik, J. Power Sources 184 (2008) 308.
[6] R. Dominko, M. Gaberscek, J. Drofenik, M. Bele, S. Pejovnik, Electrochem. Solid State Lett. 4 (2001) A187.
[7] H. Buqa, M. Holzapfel, F. Krumeich, C. Veit, P. Novák, J. Power Sources 161 (2006) 617.
[8] C.C. Li, J.T. Lee, C.Y. Lo, M.S. Wu, Electrochem. Solid State Lett. 8 (2005) A509.
[9] C.C. Li, J.T. Lee, X.W. Peng, J. Electrochem. Soc. 153 (2006) A809.
[10] S. Franger, C. Bourbon, F. Le Cras, H. Rouault, Electrochem. Solid State Lett. 5 (2002) A231–A233.
[11] S. Franger, C. Bourbon, F. Le Cras, J. Electrochem. Soc. 151 (2004) A1024–A1027.
[12] W. Porcher, P. Moreau, B. Lestriez, S. Jouanneau, D. Guyomard, Electrochem. Solid State Lett. 11 (2008) A4–A8.
[13] W. Porcher, B. Lestriez, S. Jouanneau, D. Guyomard, J. Electrochem. Soc. 156 (2009) A133–A144.
[14] T.J. Patey, A. Hintennach, L. La Mantia, P. Nov Novák, J. Power Sources 189 (2009) 590–593.
[15] M. Maccario, L. Croguennec, A. Wattiaux, E. Suard, F. Le Cras, C. Delmas, Solid State Ionics 179 (2008) 2020–2026.
[16] M. Maccario, L. Croguennec, F. Weill, F. Le Cras, C. Delmas, Solid State Ionics 179 (2008) 2383–2389.
[17] W. Porcher, P. Moreau, B. Lestriez, S. Jouanneau, F. Le Cras, D. Guyomard, Ionics 14 (2008) 583–587.
[18] J. Kim, B. Kim, J.G. Lee, J. Cho, B. Park, J. Power Sources 139 (2005) 289.
[19] M. Bele, A. Kodre, I. Arcon, J. Grdadolnik, S. Pejovnik, J.O. Besenhard, Carbon 36 (1998) 1207–1212.
[20] C.M. Gonzalez-Garcia, M.L. Gonzalez-Martin, V. Gomez-Serrano, J.M. Bruque, L. Labajos-Broncano, Langmuir 16 (2000) 3950–3956.
[21] A. Malliaris, D.T. Turner, J. Appl. Phys. 42 (1971) 614–618.
[22] D. Quemada, C. Berli, Adv. Colloid Interf. Sci. 98 (2002) 51–85.
[23] M. Yoo, C.W. Frank, S. Mori, S. Yamaguchi, Polymer 44 (2003) 4197.
[24] Z. Chen, L. Christensen, J.R. Dahn, J. Electrochem. Soc. 150 (2003) A1073.
[25] C.-C. Li, J.-T. Lee, Y.-L. Tung, C.-R. Yang, J. Mater. Sci. 42 (2007) 5773.
[26] C. Creton, E.J. Kramer, H.R. Brown, C.Y. Hui, Adv. Polym. Sci. 156 (2001) 53.
[27] D.Y.W. Yu, K. Donoue, T. Inoue, M. Fujimoto, S. Fujitani, J. Electrochem. Soc. 153 (2006) A835–A839.
[28] M. Gaberscek, M. Küzma, J. Jamnik, Phys. Chem. Chem. Phys. 9 (2007) 1815–1820.